Effect of Endothelial Progenitor Cells Transplantation on Neointimal Hyperplasia and Reendothelialization after Balloon Catheter Injury in Rat Carotid Arteries

WEI WANG
Chinese PLA General Hospital https://orcid.org/0000-0002-3117-296X
Yingqian Zhang
Chinese PLA General Hospital
Hui Hui
CASIA: Institute of Automation Chinese Academy of Sciences
Wei Tong
Chinese PLA General Hospital
Zechen Wei
CASIA: Institute of Automation Chinese Academy of Sciences
Zhongxuan Li
Chinese PLA General Hospital
Suhui Zhang
Chinese PLA General Hospital
Xin Yang
CASIA: Institute of Automation Chinese Academy of Sciences
Jie Tian
Chinese PLA General Hospital
Yundai Chen (cyundai@vip.163.com)
Chinese PLA General Hospital, Beijing

Research

Keywords: Endothelial progenitor cells, Reendothelialization, Cell transplantation

Posted Date: October 21st, 2020

DOI: https://doi.org/10.21203/rs.3.rs-92875/v1

Version of Record: A version of this preprint was published on February 3rd, 2021. See the published version at https://doi.org/10.1186/s13287-021-02135-w.

Abstract

Background: Reendothelialization is a natural pathway to inhibit neointimal hyperplasia and in-stent restenosis. Circulating endothelial progenitor cells (EPCs) derived from bone marrow might contribute to endothelial repair. However, the temporal and spatial distribution of injured vascular reendothelialization and neointimal hyperplasia in the presence of transplanted EPCs is not quite clear.

Methods: We performed a carotid balloon injury model and treated by transplantation of bone marrow-derived EPCs. To evaluate the temporal and spatial distribution of neointimal hyperplasia and reendothelialization after injury, the carotid arteries were harvested at different time points after transplantation.

Results: Transplanted EPCs labeled by PKH26 were clearly observed attaching on the injured luminal surface at day 1 post-injury. For the undamaged arteries, the transplanted EPCs never adhered to the luminal surface. From day 4 post-injury, the average value of PKH26 fluorescence decreased significantly. Although transplanted EPCs were decreased significantly at the site of injury on day 4 after transplantation, reendothelialization at the site of the injury and inhibition of neointimal hyperplasia were significantly promoted by transplanted EPCs. The degree of reendothelialization of EPC^{7d} (group of EPCs transplantation after balloon injury and harvested at day 7 post-transplantation)/EPC^{14d} was significantly better than that of the BI^{7d} (group of medium injection after balloon injury and harvested at day 7 post-injection)/BI^{14d}, and the statistical difference of neointimal hyperplasia began to appear between EPC^{14d} and BI^{14d}. The number of endothelial cells on the lumen surface of EPC^{14d} increased than that of BI^{14d}, and the number of infiltrated macrophages at the injury site decreased.

Conclusions: Transplanted EPCs had chemotactic enrichment and attached to the injured arterial intima after transplantation. Although decreased significantly at the site of injury over time after transplantation, transplanted EPCs could still promote the reendothelialization at the site of the injury and inhibition of neointimal hyperplasia.

Background

Coronary artery disease (CAD) remained the leading cause of disability and death, and has high morbidity[1, 2]. Percutaneous coronary intervention (PCI) has revolutionized the treatment of CAD, but it injured the vascular endothelial cells (VECs). Delayed reendothelialization is a critical factor of in-stent restenosis (ISR)[3–5]. The injured vascular endothelium might cause vascular inflammation which accelerates lipid deposition and thrombosis. These changes contribute to neointimal hyperplasia and ISR[6, 7]. The use of drug eluting stents (DESs) inhibits neointimal hyperplasia, but also inhibits the process of reendothelialization. ISR still occurs in approximately 10% patients in the era of DES[8]. Reendothelialization is a natural pathway to inhibit neointimal hyperplasia and ISR. It is important to accelerate reendothelialization for preventing ISR. A growing body of research has found that endothelial

progenitor cells (EPCs) might contribute to endothelial repair. EPCs capturing biomolecules were immobilized onto metal-based biomaterial surfaces to accelerate reendothelialization[9].

Some researchers suggested that circulating EPCs can not only accelerate reendothelialization by paracrine but also differentiate into mature VECs[10]. Others claimed that EPCs never differentiate into mature VECs to cover the area of injury. EPCs can only accelerate the proliferation and migration of original matured VECs nearby. Although great efforts have been taken to investigate how EPCs accelerate reendothelialization, the temporal and spatial distribution of injured vascular reendothelialization and neointimal hyperplasia in the presence of transplanted EPCs is not quite clear.

We performed a carotid balloon injury model and treated by transplantation of bone marrow-derived EPCs. For fully evaluate the spatial distribution of neointimal hyperplasia and reendothelialization after injury, the carotid arteries were harvested at different time points after transplantation.

Methods

BM-derived EPCs isolation and expansion

Sprague-Dawley (SD) rats (male, 150g, SCXK2016-0006) from Charles River Laboratories Supplier in China (Beijing, China, SCXK2016-0006) were sacrificed by cervical dislocation. The rats' tibias and femurs of both sides (4 long bones from the hind limbs) were rinsed repeatedly to obtain the bone marrow. To isolate the mononuclear cells (MNCs), Histopaque-1083 (Sigma-Aldrich, St. Louis, MO, USA) was put into use when dealing with the cell suspension with density gradient centrifugation. After isolating, mononuclear cells were seeded on a 100-mm plate at a density of 2.5×10^6 cells/cm^2. These plates were coated at 37℃ using fibronectin (R&D Systems, Minneapolis, MN, USA) 24 hours before. Cells were cultured with EGM-2 (Lonza, Walkersville, MD, USA) containing 5% fetal bovine serum. 24 hours later, gently suck the cells floating in the medium and discard them. Changed the medium daily for the first 3 days and then every 2 days. About 5 days later, cell clusters could be observed. Cells were examined under the microscope every day (IX73, Olympus, Center Valley, PA, USA) (Fig. 1A-D). A colony forming unit consists of a circular central core surrounded by elongated and spindle cells could be identified as endothelial progenitor cell colony[11]. EPCs at passage 3 were obtained and used in the further experiment.

Incorporation of Dil-Ac-LDL and lectin binding

After 8 days of culture, washed the EPCs extensively with phosphate buffer solution and subsequently stained with 1,1'-dioctadecyl-3,3,3',3'-tetramethylindocarbocyanine-labeled acetylated low-density lipoprotein (Dil-ac-LDL, Maokang Biotechnogy Co., Ltd., Shanghai, China, MP6013) at a final concentration of 10mg/L. Before Fixing the cells with 2% paraformaldehyde in PBS for 10min, the cells were incubated at 37℃ and 5% CO_2 for 4h. After fixation, dyed the cells with fluorescein isothiocyanate-

labeled Ulex europaeus agglutinin (FITC-UEA-1) (FITC-UEA-1, Maokang Biotechnogy Co., Ltd., Shanghai, China, MP6308) at a final concentration of 10mg/L. The cells were observed under the confocal fluorescent microscopy (TCS SP5 II), cells double positive for Dil-Ac-LDL and FITC-UEA-1 staining were identified as EPCs (Fig. 1E-G).

Animals and protocols

All animals were kept free of pathogen and provided clean water and rats diet for maintaining ad libitum. The final sample size was determined based on the preliminary results. SD rats (weight: 250-300g, age: 7-8 weeks, male) were obtained from the Charles River Laboratories Supplier in China (Beijing, China, SCXK2016-0006). The rats were anaesthetized with 40mg/kg bw pentobarbital via intraperitoneal injection and subject to balloon injury in the common carotid artery of the right side. Briefly, the rats were placed in supine position, the bifurcation of the right carotid artery was exposed after intravenous injection of 100 U/kg of heparin sodium via a neck midline incision. Prepared two ligatures around the external carotid artery and one ligature around the internal carotid artery. First, tied off the distal ligature around the external carotid artery to ensure that the blood flow is blocked. After that, make a temporary occlusion to the internal carotid artery and proximal side of common carotid artery, performed a transverse arteriotomy between the proximal and distal ligatures of the external carotid artery. Inserted a balloon angioplasty catheter from the incision in artery. The balloon was then inflated at 2-3 atm and passed through the artery for 3 times to ensure uniformity of the extent of the endothelium injury. After injury, tied off the proximal ligature of the external carotid artery as soon as the catheter was removed. Then the blood flow through the common and internal carotid arteries was restored. Sutured the skin with 4/0 silk. Rats received either 1×10^6 bone marrow-derived EPCs labeled by PKH-26 via intravenous tail vein injection after injury (Fig. 1H-J). Control group received a corresponding amount of EGM-2 medium. Animals were allowed to recover, Ibuprofen (15mg/kg/day) dissolved in water was provided ad libitum as a pain killer for 3 days after the balloon-injured procedure. At 1 day, 4 days, 7 days, and 14 days after balloon injury, rats were sacrificed and the common carotid arteries were harvested.

Perfusion and tissue preparation

The rats were anaesthetized with 40mg/kg bw pentobarbital via intraperitoneal injection and received 10mg/kg bw 0.1% Evans blue dye (Coolaber) by intravenous tail vein injection 30 minutes before tissue harvesting. Perfused the animals transcardially follow the sequence of 0.01M phosphate-buffered saline (PBS) (P3813, Sigma-Aldrich) and 4% paraformaldehyde (PFA; 158127, Sigma-Aldrich) in PBS. The common carotid arteries were harvested and fixed in 4% PFA at 4℃ at least 24 hours before clearing.

Tissue clearing procedure

The common carotid artery embedded in 1% agar was dehydrated with methanol solutions (mixed with PBS) follow the sequence of concentrations 25, 50, 75, and 100 volume % for 3 hours each. Benzyl alcohol and benzyl benzoate was used in a ratio of one to three as a refractive index matching solution. All steps were performed at room temperature and keep shaking slightly. Finally, placed the sample in the dark by covering aluminum foil. The artery was observed by light-sheet microscopy.

Light-sheet microscopy

Arteries were observed under the light-sheet fluorescence microscope (LaVision Biotec, Bielefeld, Germany). We used a 2.5x objective lens (Mv PLAPO 2VC, Olympus) or a 4x objective lens (Mv PLAPO 2VC, Olympus) covered with a 6mm working distance dipping cap. A supercontinuum white light laser (SuperK EXTREME 80 mHz VIS with wavelength from 400 to 2400nm, NKT Photonics, Cologne, Germany) was chosen as a laser source. To observe the cell distribution and artery morphology, the filters were set as 551/40nm excitation and 567/50nm emission for PKH26 and 640/30nm excitation and 690/50nm emission for Evans blue. The step size was set to 5μm. Carotid artery scanning range was set to 1mm. 3D projections of the tagged image file format (TIFF) images of the artery were obtained by using Imaris software (Bitplane, Oxford Instruments Company).

Image Processing

Images of light-sheet fluorescence microscopy were stored as 16 bit ome.tif stacks. Considering that the range of pixel values of different images is inconsistent, we firstly normalize all the image values to [0,255]. Secondly, the threshold value is obtained by using the non-invasive group, which is the maximum value of the image. Then, images of other groups are processed, with the pixel value less than the threshold setting to zero. The average value without zero is the sum of processed pixels divided by the number of non-zero pixels. All the image values would be normalized to [0,1] before the final statistical analysis. Images of hematoxylin and eosin (H&E) and immunofluorescence were analyzed using tools of ImageJ (version 1.52a, Wayne Rasband, National Institutes of Health, USA).

Morphometric analysis

Carotid arteries were trimmed and paraffin embedded in the Histology and Comparative Pathology Facility. Paraffin blocks were trimmed with a microtome until a full cross-section of the artery was visualized. Tissue sections of 5μm thick from three different regions of the artery were collected. Arterial sections were dyed with H&E and photographed with a Leica DM3000 microscope. For immunofluorescence, artery sections were deparaffinized, rehydrated, and antigen retrieved by a sodium citrate method (Vector Labs H-3300). Arteries were blocked with PBS containing 0.3% triton-X-100 and 5% normal goat serum for one hour at room temperature, and incubated with primary antibodies in PBS containing 0.3% triton-X-100 and 2% bovine serum albumin overnight at 4°C. After washing, sections

were incubated with fluorochrome-conjugated secondary antibodies for one hour at room temperature. After washing, arterial sections were stained with DAPI (4',6-diamidino-2-phenylindole) using FLUORO-GEL II with DAPI (Beyotime, C1005). Images were taken with a Leica DM3000 microscope. Antibodies used were Rabbit anti-CD31 antibody(Abcam, ab24590, 1:50 dilution), and goat anti-rabbit IgG (Boster, BA1032, 1:400 dilution).

Statistical analysis

Continuous variables consistent a normal distribution were expressed as mean ± standard deviation (SD). Multiple group comparisons were performed using a one-way ANOVA, followed by a post hoc analysis using the least significant difference (LSD) t-test or Dunnett's T3 post-hoc test using Welch's ANOVA. Comparisons between two independent groups were analyzed using Student's t-test. Two-sided tests were used throughout the experiment. $P < 0.05$ was considered statistically significant. ALL data were analyzed using GraphPad Prism-8 statistic software (La Jolla, CA).

Results

The effect of EPCs transplantation on neointimal hyperplasia in balloon-injured rat carotid artery

The volume of neointimal was increased from BI^{1d} (group of medium injection after balloon injury and harvested at day 1 post-injection), BI^{4d}, BI^{7d}, to BI^{14d}. EPCs were transplanted after injury immediately, the volume of neointima was increased from EPC^{1d} (group of EPCs transplantation after balloon injury and harvested at day 1 post-transplantation), EPC^{4d}, EPC^{7d}, to EPC^{14d}. Compared with BI^{14d} (0.107 ± 0.008), the neointimal volume of EPC^{14d} (0.084 ± 0.009) was significantly smaller ($P = 0.027$), while there was no significant difference between EPC^{1d} and BI^{1d} (0.009 ± 0.001 vs. 0.010 ± 0.001, $P = 0.525$), EPC^{4d} and BI^{4d} (0.030 ± 0.003 vs. 0.035 ± 0.004, $P = 0.154$), EPC^{7d} and BI^{7d} (0.033 ± 0.009 vs. 0.044 ± 0.003, $P = 0.109$) (Fig. 2A-B).

We also compared the neointimal area between EPCs transplantation group and the non-transplantation group at day 14 post-injury via H&E staining. The area of neointimal in EPC^{14d} decreased significantly compared with BI^{14d} (0.066 ± 0.018 vs. 0.137 ± 0.008, $P = 0.040$) (Fig. 3A-B).

Three-dimensional distribution of transplanted EPCs and the effect of EPCs transplantation on reendothelialization

Also, we sought to characterize the reendothelialization after injury of the carotid artery using three-dimensional (3D) evaluation. The distribution of transplanted EPCs change in three dimensions over time, but the impairment of endothelial integrity was typically measured with cross- or longitudinal sections

and subsequent histological analysis[12–14]. Transplanted EPCs labeled by PKH26 could be observed in the 551 nm channel under a light-sheet microscopy, and attaching to the luminal surface of injured vessel at day 1 post-injury. While no labeled cells attached to the uninjured side. From day 4 post-injury, the average value of PKH26 fluorescence decreased significantly on the luminal surface of injured vessel. The average value of PKH26 fluorescence were highest in EPC^{1d} (0.175 ± 0.434), lowest in EPC^{14d} (0.073 ± 0.030), significantly higher in EPC^{1d} than EPC^{4d} (0.175 ± 0.434 vs. 0.095 ± 0.041, $P = 0.023$)/ EPC^{7d} (0.175 ± 0.434 vs. 0.083 ± 0.020, $P = 0.012$)/ EPC^{14d} (0.175 ± 0.434 vs. 0.073 ± 0.030, $P = 0.007$). Evans blue could penetrate the areas where the endothelium is permeable and stain the injured surface blue. An intact endothelium could maintain an unstained surface[15]. The injured endothelium labeled by Evans blue could be observed in the 611 nm channel under a light-sheet microscopy. The average value of Evans blue fluorescence decreased from BI^{1d} (0.411 ± 0.088)/EPC^{1d} (0.352 ± 0.031) to BI^{14d} (0.344 ± 0.022)/EPC^{14d} (0.195 ± 0.030). The average value of Evans blue fluorescence was significantly larger in BI^{14d} than EPC^{14d} (0.344 ± 0.022 vs. 0.195 ± 0.030, $P = 0.002$), and in BI^{7d} and EPC^{7d} (0.335 ± 0.095 vs. 0.169 ± 0.003, $P = 0.039$), they showed no difference between BI^{1d} and EPC^{1d} (0.411 ± 0.088 vs. 0.352 ± 0.031, $P = 0.340$), or BI^{4d} and EPC^{4d} (0.378 ± 0.029 vs. 0.348 ± 0.010, $P = 0.163$) (Fig. 4A-D).

we also compared CD31 positive cell on luminal surface at day 14 post-injury between the EPCs transplanted and non-transplanted groups via immunofluorescence. The CD31 positive cell in EPC^{14d} were more than BI^{14d} (18.843 ± 3.454 vs. 4.115 ± 0.269, $P < 0.001$) (Fig. 5A-B), which is consistent with the results of 3D evaluation.

we evaluated the degree of macrophage infiltration in right common carotid arteries at day 14 post-injury by comparing the CD68 positive cell via immunofluorescence. The CD68 positive cell in EPC^{14d} were less than BI^{14d} (12.774 ± 3.561 vs. 32.259 ± 10.125, $P = 0.002$) (Fig. 6A-B).

Discussion

This study demonstrated that transplanted EPCs have chemotactic enrichment and can be attached to the injured site after transplantation. The transplanted cells become less visible at the site of injury from day 4 post-injury. Although the average value of PKH26 fluorescence decreased significantly on the vascular lumen from the 4th day after transplantation, reendothelialization of injured vessels was significantly accelerated and neointimal hyperplasia was significantly inhibited in the EPCs transplanted group in comparison with the non-transplanted group.

We used a rat carotid balloon injury model, a commonly used injury model[16–18], to induce neointimal hyperplasia in rats. The mechanism of the injury was similar with that of percutaneous transluminal coronary angioplasty. Neointima formation is a process in three dimensions. But it is typically measured in two dimensions without an accurate 3D reconstruction[19–21]. Traditional 2D analyses cannot fully evaluate the spatial distribution of neointimal hyperplasia. Selection bias will be made, and

underestimation or overestimation will occur. For its irregular geometry, the process of neointimal hyperplasia should be evaluated in three dimensions.

Light-sheet microscopy has been used to process 3D reconstruction of cardiac structures in zebrafish and murine[22–25]. While it failed in imaging the vascular structure alone due to its low resolution. Photons and molecular probes are difficult to approach tissues because of the diffusion-barrier properties of lipid bilayers and the light scattering properties of lipid-water interface[26]. People try to use a newly created technique, called tissue clearing, to ensure the density of the scatterer is highly uniform. With tissue clearing, lateral scattering is minimal and all wavelengths of light could pass through the tissue[27]. Light-sheet microscopy in combination with tissue clearing has been previously used to characterize the murine brain and cochleae as well as atherosclerosis plaque[26, 28, 29]. Cleared with benzyl alcohol/benzyl benzoate is a kind of tissue clearing methods called BABB. It have been applied to produce 3D images of tissues including marine embryo, brain, skin and human gingiva[30–33]. However, this technique has not been used in the study of the spatial distribution of endothelium injury, neointimal hyperplasia and transplanted EPCs distribution in balloon-injured carotid arteries.

Here, we have applied the BABB tissue clearing method in combination with light-sheet microscopy for 3D evaluation of pathophysiological events after injury. Using this method, we calculate its volume, not just its area. With our method we found that the degree of neointimal hyperplasia changed with respect to the recovery time after surgery. The volume of neointimal was increased from BI^{1d}, BI^{4d}, BI^{7d}, to BI^{14d}. With EPCs transplantation, the volume of neointimal was also increased from EPC^{1d}, EPC^{4d}, EPC^{7d}, to EPC^{14d}. Restoration of intact endothelium after injury is of great significance for the prevention of neointimal hyperplasia and stent thrombosis[34, 35]. Reendothelialization could be accelerated by EPCs transplantation[36–38]. The neointimal volume of EPC^{14d} was significantly smaller than BI^{14d}, while there was no significant difference between EPC^{1d} and BI^{1d}, EPC^{4d} and BI^{4d}, or EPC^{7d} and BI^{7d}.

To explore the mechanism of transplanted EPCs accelerating reendothelialization, previous studies have different conclusion. Hagensen et al. suggested that the migration of adjacent arterial endothelial cells is the only source of reendothelialization[39]. However, other scholars declared that transplanting EPCs could not only promote reendothelialization through paracrine modes of action, but also differentiate into mature ECs[40, 41]. Assessment of transplanted EPCs and reendothelialization requires sequential cross- or longitudinal sectioning of the vessels[42–45], but not every section could be chosen to stain and quantify[46–48]. The irregular geometry of the cell distribution requires accurate tools. Developmental assessment of the relationship between transplanted EPCs and reendothelialization requires evaluating morphogenesis of injured vessels in the context of three dimensions.

Transplanted EPCs labeled by PKH26 were clearly observed attaching on the injured luminal surface at day 1 post-injury. For the undamaged arteries, the transplanted EPCs never adhered to the luminal surface. Our results support the idea that transplanted EPCs have chemotactic enrichment and adhere to the site of endothelial injury. From day 4 post-injury, the average value of PKH26 fluorescence decreased significantly. PKH26 could be positive on the newborn cell membrane with cell proliferation, while PKH26

did not appear in the reendothelialization region from day 4 post-injury, indicating that the PKH26 labeled-EPCs did not proliferate and differentiate into mature endothelial cells to cover the injured endothelium. Although transplanted EPCs were decreased significantly at the site of injury on day 4 after transplantation, reendothelialization at the site of the injury and inhibition of neointimal hyperplasia were significantly promoted by transplanted EPCs. The degree of reendothelialization of EPC^{7d}/EPC^{14d} was significantly better than that of the BI^{7d}/BI^{14d}, and the statistical difference of neointimal hyperplasia began to appear between EPC^{14d} and BI^{14d}. The number of endothelial cells on the lumen surface of EPC^{14d} increased than that of BI^{14d}, and the number of infiltrated macrophages at the injury site decreased. The mechanism by which EPCs can facilitate reendothelialization of injured vessel is more likely to be promoting the proliferation of adjacent endothelial cells to cover the damaged area through paracrine cytokines.

There are limitations to the present work. First, we used only a segment of the right common carotid artery instead of the entire artery since the size of the light-sheet microscopy was limited, and the entire common carotid artery will be analyzed in our future study. Second, our methodology requires harvesting the vessel of interest, and therefore, does not allow sequential assessments in the same animal.

Conclusions

We find that transplanted EPCs can attenuate neointimal hyperplasia and accelerated reendothelialization after endothelium injury. And the possible mechanism underlying it is that transplanted EPCs. Transplanted EPCs had chemotactic enrichment and attached on the injured luminal surface, and promoting the proliferation of adjacent endothelial cells to cover the damaged area through paracrine cytokines, but did not differentiate into mature endothelial cells.

Abbreviations

EPCs: Endothelial progenitor cells; CAD: Coronary artery disease; PCI: Percutaneous coronary intervention; VECs: Vascular endothelial cells; ISR: In-stent restenosis; DESs: Drug eluting stents; 3D: Three-dimensional; SD rats: Sprague-Dawley rats; MNCs: Mononuclear cells; Dil-ac-LDL: 1,1’-dioctadecyl-3,3,3’,3’-tetramethylindocarbocyanine-labeled acetylated low-density lipoprotein; FITC-UEA-1: Fluorescein isothiocyanate-labeled Ulex europaeus agglutinin; PBS: Phosphate-buffered saline; TIFF: Tagged image file format; H&E: Hematoxylin and eosin; PFA: paraformaldehyde; DAPI: 4',6-diamidino-2-phenylindole.

Declarations

Ethics approval

Animal Research Committee of Chinese PLA General Hospital have approved all experiments. All the animal experiments were conducted in accordance with the Guide for the Care and Use of Laboratory Animals published by the US National Institutes of Health (NIH Publication No.85-23, revised 1996).

Consent for publication

Not applicable.

Availability of data and materials

All data generated or analyzed during this study are included in this article and its supplementary information files.

Competing interests

The authors declare that they have no competing interert.

Funding

This work was supported in part by the National Key Research and Development Program of China under Grant 2017YFA0700401, 2016YFC0103803; the National Natural Science Foundation of China (Grant Nos. 81800221, 81671731, 81827808, 81671851, 81870178, 81527805, 81971680, 81227901); the Capital Clinical Feature Research Project (Grant Nos. Z171100001017158); the CAS Strategic Priority Research Program under Grant XDB32030200 and the CAS Scientific Instrument R&D Program under Grant YJKYYQ20170075, the Youth Innovation Promotion Association under Grant 2018167, of the Chinese Academy of Sciences.

Authors’ contributions

All authors assisted in this study. WW, YZ, and HH designed and performed experiments, analyzed and interpreted data, prepared figures, and wrote the manuscript. WT, ZL, SZ and XY performed experiments. ZW analyzed and interpreted data, and edited the manuscript. JT conceptualized studies, designed experiments, evaluated data, and edited the manuscript. YC conceptualized studies, designed and performed experiments, evaluated all data, and wrote the manuscript.

Acknowledgements

Not applicable.

References

1. Timmis A, Townsend N, Gale C, Grobbee R, Maniadakis N, Flather M, et al. European Society of Cardiology: Cardiovascular Disease Statistics 2017. Eur Heart J. 2018;39(7):508-79.

2. Benjamin EJ, Muntner P, Alonso A, Bittencourt MS, Callaway CW, Carson AP, et al. Heart Disease and Stroke Statistics-2019 Update: A Report From the American Heart Association. Circulation. 2019;139(10):e56-e528.
3. Tsigkas GG, Karantalis V, Hahalis G, Alexopoulos D. Stent restenosis, pathophysiology and treatment options: a 2010 update. Hellenic J Cardiol. 2011;52(2):149-57.
4. Collins MJ, Li X, Lv W, Yang C, Protack CD, Muto A, et al. Therapeutic strategies to combat neointimal hyperplasia in vascular grafts. Expert Rev Cardiovasc Ther. 2012;10(5):635-47.
5. Huang YH, Xu Q, Shen T, Li JK, Sheng JY, Shi HJ. Prevention of in-stent restenosis with endothelial progenitor cell (EPC) capture stent placement combined with regional EPC transplantation: An atherosclerotic rabbit model. Cardiol J. 2019;26(3):283-91.
6. Dangas GD, Claessen BE, Caixeta A, Sanidas EA, Mintz GS, Mehran R. In-stent restenosis in the drug-eluting stent era. J Am Coll Cardiol. 2010;56(23):1897-907.
7. Ding H, Zhang T, Du Y, Liu B, Liu Y, Wang F. HUCMNCs protect vascular endothelium and prevent ISR after endovascular interventional therapy for vascular diseases in T2DM rabbits. Mol Cell Biochem. 2017;433(1-2):161-7.
8. Kokkinidis DG, Waldo SW, Armstrong EJ. Treatment of coronary artery in-stent restenosis. Expert Rev Cardiovasc Ther. 2017;15(3):191-202.
9. Cui Y, Zhou F, Wei L, Song Q, Tan J, Zeng Z, et al. In Situ Endothelialization Promoted by SEMA4D and CXCL12 for Titanium-Based Biomaterials. Seminars in thrombosis and hemostasis. 2018;44(1):70-80.
10. Rana D, Kumar A, Sharma S. Endothelial Progenitor Cells as Molecular Targets in Vascular Senescence and Repair. Current stem cell research & therapy. 2018;13(6):438-46.
11. Powell TM, Paul JD, Hill JM, Thompson M, Benjamin M, Rodrigo M, et al. Granulocyte colony-stimulating factor mobilizes functional endothelial progenitor cells in patients with coronary artery disease. Arterioscler Thromb Vasc Biol. 2005;25(2):296-301.
12. Tang F, Liu M, Zeng O, Tan W, Long J, Liu S, et al. Gefitinib-coated balloon inhibits the excessive hyperplasia of intima after vascular injuries through PI3K/AKT pathway. Technol Health Care. 2019;27(S1):331-43.
13. Gong Z, Han Y, Wu L, Xia T, Ren H, Yang D, et al. Translocator protein 18 kDa ligand alleviates neointimal hyperplasia in the diabetic rat artery injury model via activating PKG. Life Sci. 2019;221:72-82.
14. Fan Y, Chen Y, Zhang J, Yang F, Hu Y, Zhang L, et al. Protective Role of RNA Helicase DEAD-Box Protein 5 in Smooth Muscle Cell Proliferation and Vascular Remodeling. Circ Res. 2019;124(10):e84-e100.
15. Autar A, Taha A, van Duin R, Krabbendam-Peters I, Duncker DJ, Zijlstra F, et al. Endovascular procedures cause transient endothelial injury but do not disrupt mature neointima in Drug Eluting Stents. Sci Rep. 2020;10(1):2173.

16. Gao Y, Gao CY, Zhu P, Xu SF, Luo YM, Deng J, et al. Ginsenoside Re inhibits vascular neointimal hyperplasia in balloon-injured carotid arteries through activating the eNOS/NO/cGMP pathway in rats. Biomed Pharmacother. 2018;106:1091-7.
17. Qiu L, Xu C, Chen J, Li Q, Jiang H. Downregulation of the transcriptional co-activator PCAF inhibits the proliferation and migration of vascular smooth muscle cells and attenuates NF-κB-mediated inflammatory responses. Biochem Biophys Res Commun. 2019;513(1):41-8.
18. Fan T, He J, Yin Y, Wen K, Kang Y, Zhao H, et al. Dioscin inhibits intimal hyperplasia in rat carotid artery balloon injury model through inhibition of the MAPK-FoxM1 pathway. Eur J Pharmacol. 2019;854:213-23.
19. Zhang J, Chen J, Yang J, Xu C, Hu Q, Wu H, et al. Suv39h1 downregulation inhibits neointimal hyperplasia after vascular injury. Atherosclerosis. 2019;288:76-84.
20. Duan Y, Zhang Y, Qu C, Yu W, Tana, Shen C. CKLF1 aggravates neointimal hyperplasia by inhibiting apoptosis of vascular smooth muscle cells through PI3K/AKT/NF-κB signaling. Biomed Pharmacother. 2019;117:108986.
21. Marshall AP, Luo W, Wang XL, Lin T, Cai Y, Guzman RJ. Medial artery calcification increases neointimal hyperplasia after balloon injury. Sci Rep. 2019;9(1):8193.
22. Ding Y, Lee J, Ma J, Sung K, Yokota T, Singh N, et al. Light-sheet fluorescence imaging to localize cardiac lineage and protein distribution. Sci Rep. 2017;7:42209.
23. Ding Y, Ma J, Langenbacher AD, Baek KI, Lee J, Chang CC, et al. Multiscale light-sheet for rapid imaging of cardiopulmonary system. JCI Insight. 2018;3(16):e121396.
24. Packard RRS, Baek KI, Beebe T, Jen N, Ding Y, Shi F, et al. Automated Segmentation of Light-Sheet Fluorescent Imaging to Characterize Experimental Doxorubicin-Induced Cardiac Injury and Repair. Sci Rep. 2017;7(1):8603.
25. Merz SF, Korste S, Bornemann L, Michel L, Stock P, Squire A, et al. Contemporaneous 3D characterization of acute and chronic myocardial I/R injury and response. Nat Commun. 2019;10(1):2312.
26. Chung K, Wallace J, Kim SY, Kalyanasundaram S, Andalman AS, Davidson TJ, et al. Structural and molecular interrogation of intact biological systems. Nature. 2013;497(7449):332-7.
27. Richardson DS, Lichtman JW. Clarifying Tissue Clearing. Cell. 2015;162(2):246-57.
28. Becher T, Riascos-Bernal DF, Kramer DJ, Almonte VM, Chi J, Tong T, et al. Three-Dimensional Imaging Provides Detailed Atherosclerotic Plaque Morphology and Reveals Angiogenesis After Carotid Artery Ligation. Circ Res. 2020;126(5):619-32.
29. Dai M, Yang Y, Omelchenko I, Nuttall AL, Kachelmeier A, Xiu R, et al. Bone marrow cell recruitment mediated by inducible nitric oxide synthase/stromal cell-derived factor-1alpha signaling repairs the acoustically damaged cochlear blood-labyrinth barrier. Am J Pathol. 2010;177(6):3089-99.
30. Ramirez A, Astrof S. Visualization and Analysis of Pharyngeal Arch Arteries using Whole-mount Immunohistochemistry and 3D Reconstruction. J Vis Exp. 2020;157:e60797.

31. Foster DS, Nguyen AT, Chinta M, Salhotra A, Jones RE, Mascharak S, et al. A Clearing Technique to Enhance Endogenous Fluorophores in Skin and Soft Tissue. Sci Rep. 2019;9(1):15791.
32. Azaripour A, Lagerweij T, Scharfbillig C, Jadczak AE, Swaan BV, Molenaar M, et al. Three-dimensional histochemistry and imaging of human gingiva. Sci Rep. 2018;8(1):1647.
33. Zucker RM, Rogers JM. Confocal Laser Scanning Microscopy of Morphology and Apoptosis in Organogenesis-Stage Mouse Embryos. Methods Mol Biol. 2019;1965:297-311.
34. Zhang YQ, Tian F, Zhou Y, Chen YD, Li B, Ma Q, et al. Nicorandil attenuates carotid intimal hyperplasia after balloon catheter injury in diabetic rats. Cardiovasc Diabetol. 2016;15:62.
35. Ma X, Hibbert B, Dhaliwal B, Seibert T, Chen YX, Zhao X, et al. Delayed re-endothelialization with rapamycin-coated stents is rescued by the addition of a glycogen synthase kinase-3beta inhibitor. Cardiovasc Res. 2010;86(2):338-45.
36. Sheu JJ, Hsiao HY, Chung SY, Chua S, Chen KH, Sung PH, et al. Endothelial progenitor cells, rosuvastatin and valsartan have a comparable effect on repair of balloon-denudated carotid artery injury. Am J Transl Res. 2019;11(3):1282-98.
37. Hu H, Wang B, Jiang C, Li R, Zhao J. Endothelial progenitor cell-derived exosomes facilitate vascular endothelial cell repair through shuttling miR-21-5p to modulate Thrombospondin-1 expression. Clin Sci (Lond). 2019;133(14):1629-44.
38. Iso Y, Usui S, Toyoda M, Spees JL, Umezawa A, Suzuki H. Bone marrow-derived mesenchymal stem cells inhibit vascular smooth muscle cell proliferation and neointimal hyperplasia after arterial injury in rats. Biochem Biophys Rep. 2018;16:79-87.
39. Hagensen MK, Shim J, Thim T, Falk E, Bentzon JF. Circulating endothelial progenitor cells do not contribute to plaque endothelium in murine atherosclerosis. Circulation. 2010;121(7):898-905.
40. Li L, Liu H, Xu C, Deng M, Song M, Yu X, et al. VEGF promotes endothelial progenitor cell differentiation and vascular repair through connexin 43. Stem cell research & therapy. 2017;8(1):237.
41. Ke X, Zou J, Hu Q, Wang X, Hu C, Yang R, et al. Hydrogen Sulfide-Preconditioning of Human Endothelial Progenitor Cells Transplantation Improves Re-Endothelialization in Nude Mice with Carotid Artery Injury. Cellular physiology and biochemistry : international journal of experimental cellular physiology, biochemistry, and pharmacology. 2017;43(1):308-19.
42. Huang B, Hu P, Hu A, Li Y, Shi W, Huang J, et al. Naringenin attenuates carotid restenosis in rats after balloon injury through its anti-inflammation and anti-oxidative effects via the RIP1-RIP3-MLKL signaling pathway. Eur J Pharmacol. 2019;855:167-74.
43. Tawa M, Shimosato T, Sakonjo H, Masuoka T, Nishio M, Ishibashi T, et al. Chronological Change of Vascular Reactivity to cGMP Generators in the Balloon-Injured Rat Carotid Artery. J Vasc Res. 2019;56(3):109-16.
44. Yang N, Dong B, Yang J, Li Y, Kou L, Liu Y, et al. Effects of Rosuvastatin on Apolipoprotein J in Balloon-Injured Carotid Artery in Rats. Arq Bras Cardiol. 2018;111(4):562-8.
45. Song T, Zhao J, Jiang T, Jin X, Li Y, Liu X. Formononetin protects against balloon injury-induced neointima formation in rats by regulating proliferation and migration of vascular smooth muscle

cells via the TGF-β1/Smad3 signaling pathway. Int J Mol Med. 2018;42(4):2155-62.

46. Lin JS, Wang CJ, Li WT. Photodynamic therapy of balloon-injured rat carotid arteries using indocyanine green. Lasers Med Sci. 2018;33(5):1123-30.
47. Jung SH, Lee GB, Ryu Y, Cui L, Lee HM, Kim J, et al. Inhibitory effects of scoparone from chestnut inner shell on platelet-derived growth factor-BB-induced vascular smooth muscle cell migration and vascular neointima hyperplasia. J Sci Food Agric. 2019;99(9):4397-406.
48. Zhang WX, Tai GJ, Li XX, Xu M. Inhibition of neointima hyperplasia by the combined therapy of linagliptin and metformin via AMPK/Nox4 signaling in diabetic rats. Free Radic Biol Med. 2019;143:153-63.

Figures

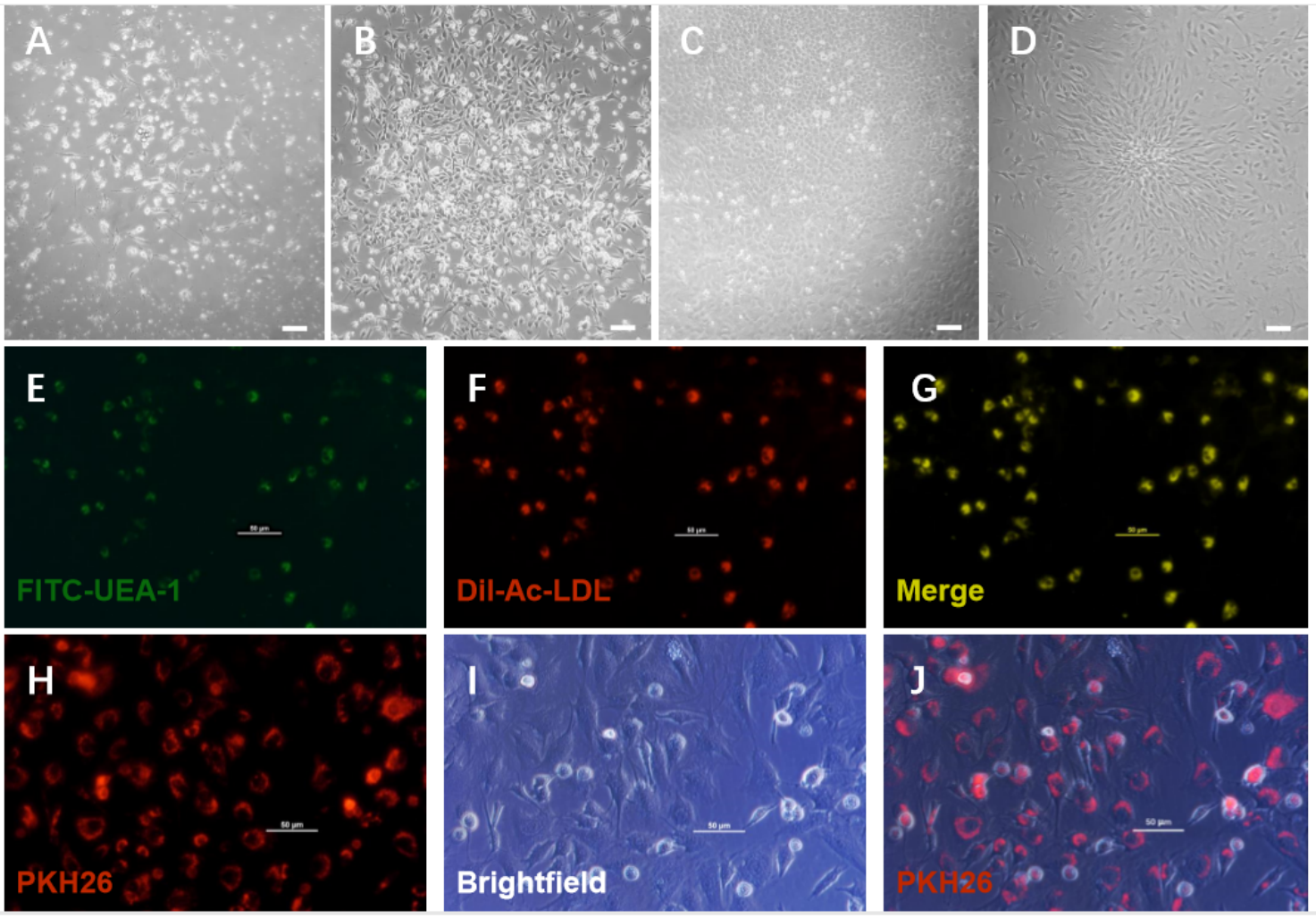

Figure 1

A-J Characterization and labeling of bone marrow-derived EPCs. (A) Adherent cells formed a cluster at day 5 of culture. (B) Cell cluster grew into a colony at day 7 of culture. (C) The cobblestone-shaped cell colony appeared at day 8 of culture. (D) The typical colonies, consisted of a central core of rounded cells

surrounded by spindle-shaped cells, appeared at day 2 post-passage. Scale bar = 100μm (A-D). (E) Green fluorescence represents cells positive for FITC-UEA-1. (F) Red fluorescence represents cells positive for Dil-ac-LDL. (G) Yellow fluorescence represents differentiated endothelial progenitor cell-like adherent cells that were double-positive for uptake of Dil-ac-LDL and binding with FITC-UEA-1. The double-positive cells accounted for 85% of the total. (H-J) PKH-26-stained bone marrow-derived EPCs injected via tail vein after balloon injury could be monitored during the period of EPCs proliferation. Scale bar = 50μm (E-J).

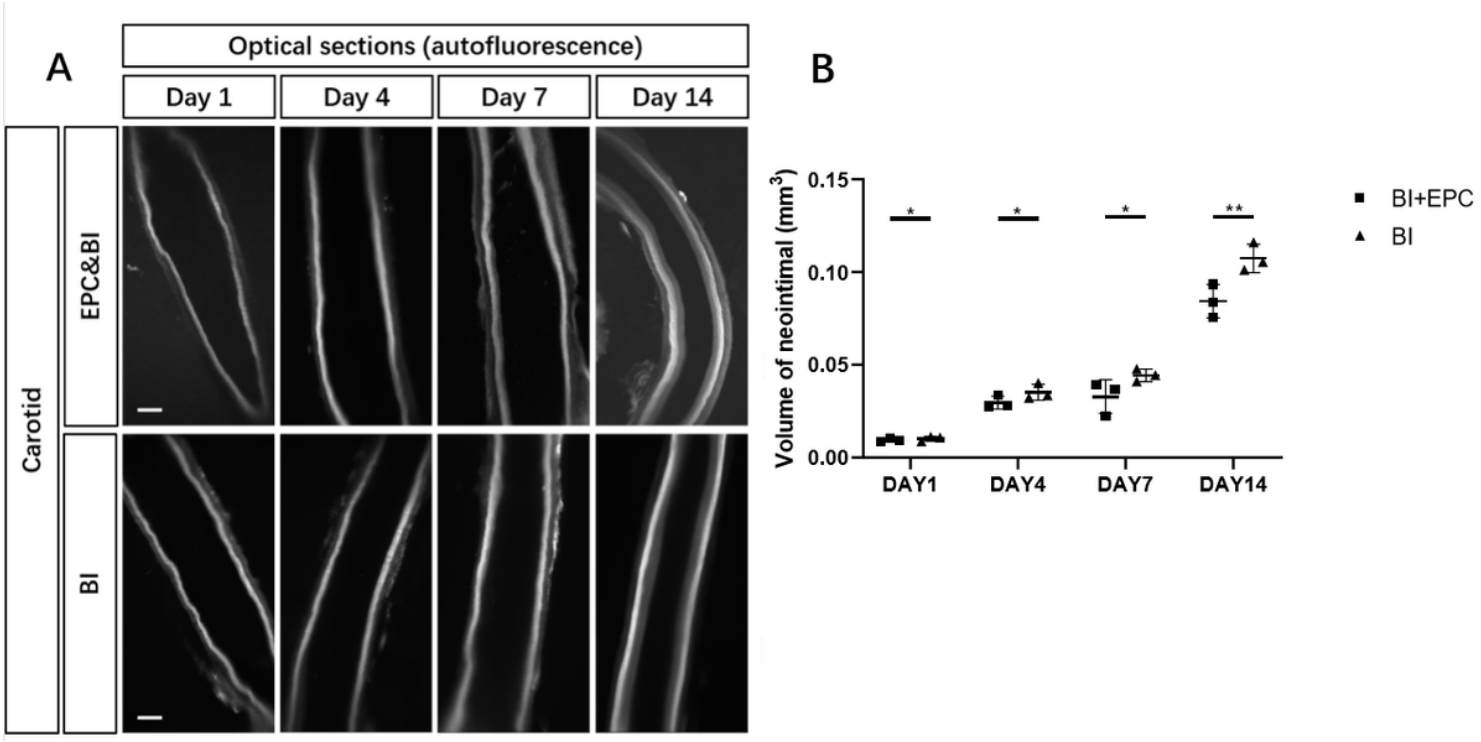

Figure 2

A-B Neointimal hyperplasia at different time points after balloon injury in different groups. (A) Autofluorescence of neointimal hyperplasia on the optical sections from each group at different time points. Scale bar=250μm. (B) Neointimal volume of different groups on day 1 post-injury, day 4 post-injury, day 7 post-injury and day 14 post-injury; data shown as mean±SEM, analyzed by independent student's t-test, n=3. *No statistical difference, **P<0.05, ***P<0.01 vs BI group. BI=balloon injured; BI+EPC=EPC administration after balloon injured.

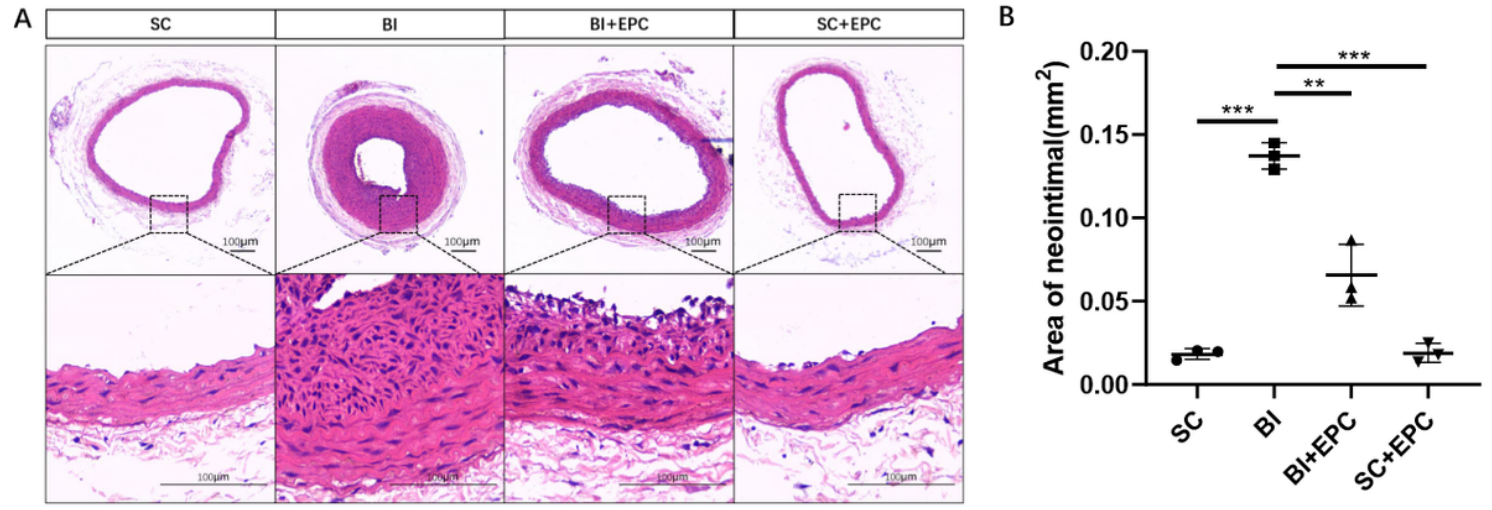

Figure 3

A-B EPCs translation attenuates neointimal hyperplasia after balloon-injured. (A) Cross sections of carotid arteries stained with H&E in different groups at day 14 post-injury. (B) Neointimal area of different groups; data shown as mean±SEM, analyzed by Welch's ANOVA with Dunnett's T3 post-hoc test, n=3. *No statistical difference, **P<0.05, ***P<0.01 vs BI group. SC=sham-operated control; BI=balloon injured; EPC&BI=EPC administration after balloon injured; EPC&SC=EPC administration after sham-operated.

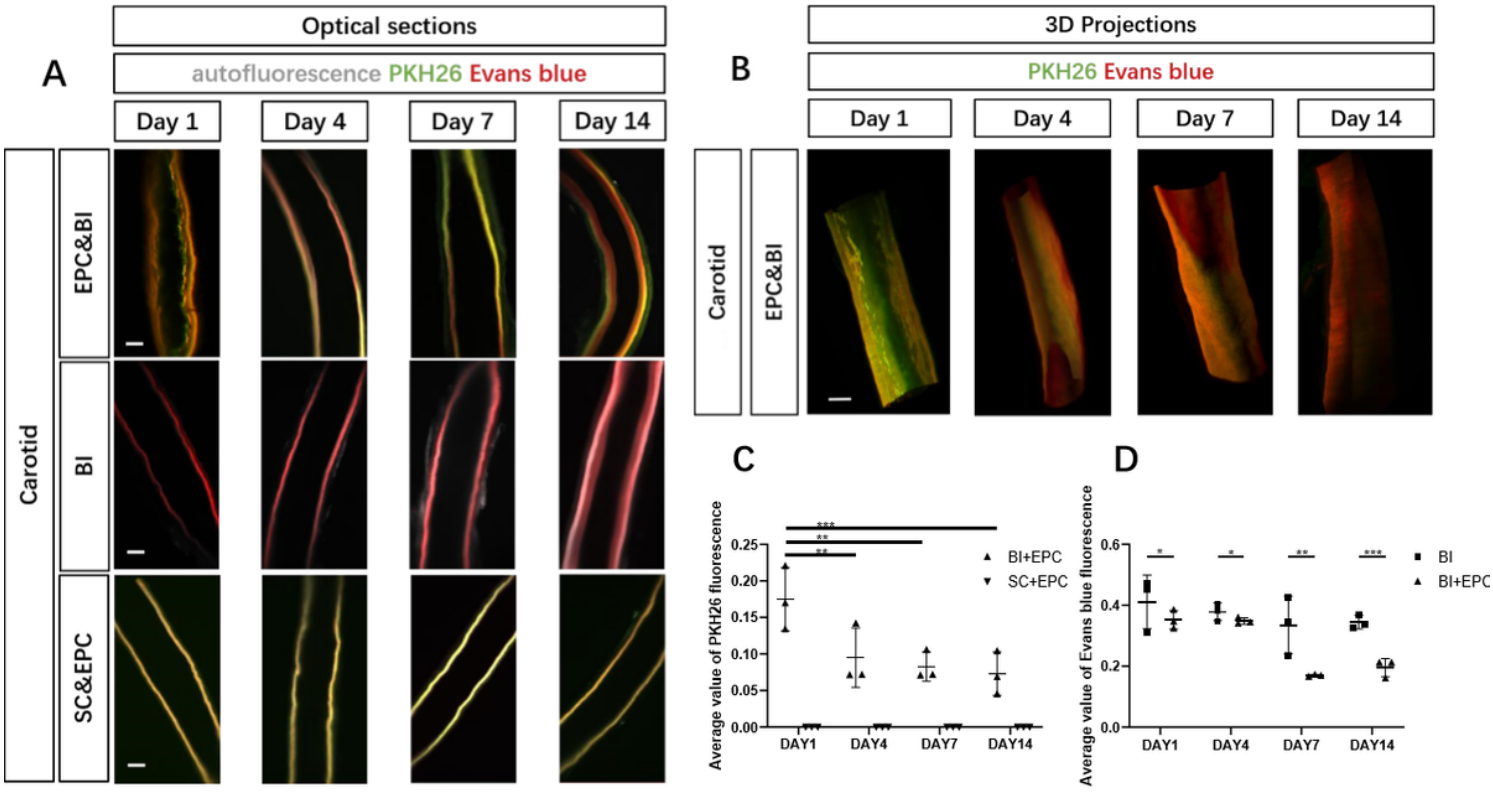

Figure 4

A-D Changes in the distribution of transplanted EPCs and injured endothelium in carotid artery. (A) Optical sections of carotid arteries. scale bar=250μm. (B) Three dimensional projections of carotid arteries. scale bar=500μm. (C) The average value of PKH26 fluorescence from labeled transplanted EPCs at different time points after injury or not; data shown as mean±SEM, analyzed by one-way ANOVA with LSD post-hoc comparisons, n=3. (D) The average value of Evans blue fluorescence from injured endothelium at different time points after injury; data shown as mean±SEM, analyzed by independent student's t-test, n=3. *No statistical difference, **P<0.05, ***P<0.01. BI=balloon injured; EPC&BI=EPC administration after balloon injured; EPC&SC=EPC administration after sham-operated.

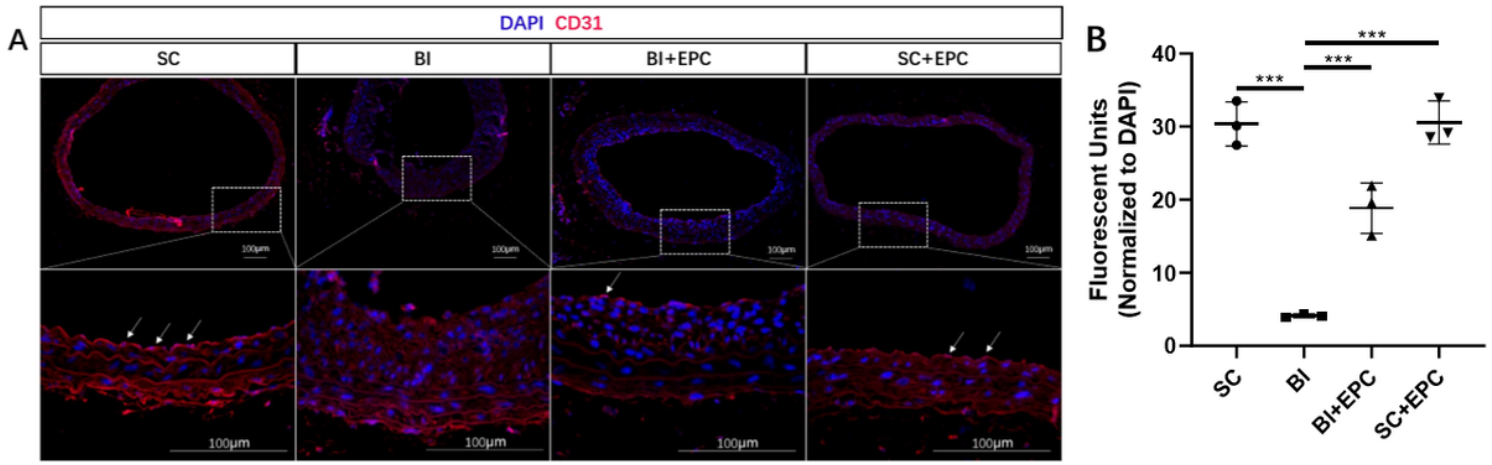

Figure 5

A-B Immunostaining of CD31 in lumen surface of different groups. (A) Immunostaining of CD31 in lumen surface of different groups. Arrows indicate endothelial cells. (B) Quantification of CD31 staining from images in (A); data shown as mean±SEM, analyzed by one-way ANOVA with LSD post-hoc comparisons, n=3. *No statistical difference, **P<0.05, ***P<0.01 vs BI group. SC=sham-operated control; BI=balloon injured; EPC&BI=EPC administration after balloon injured; EPC&SC=EPC administration after sham-operated.

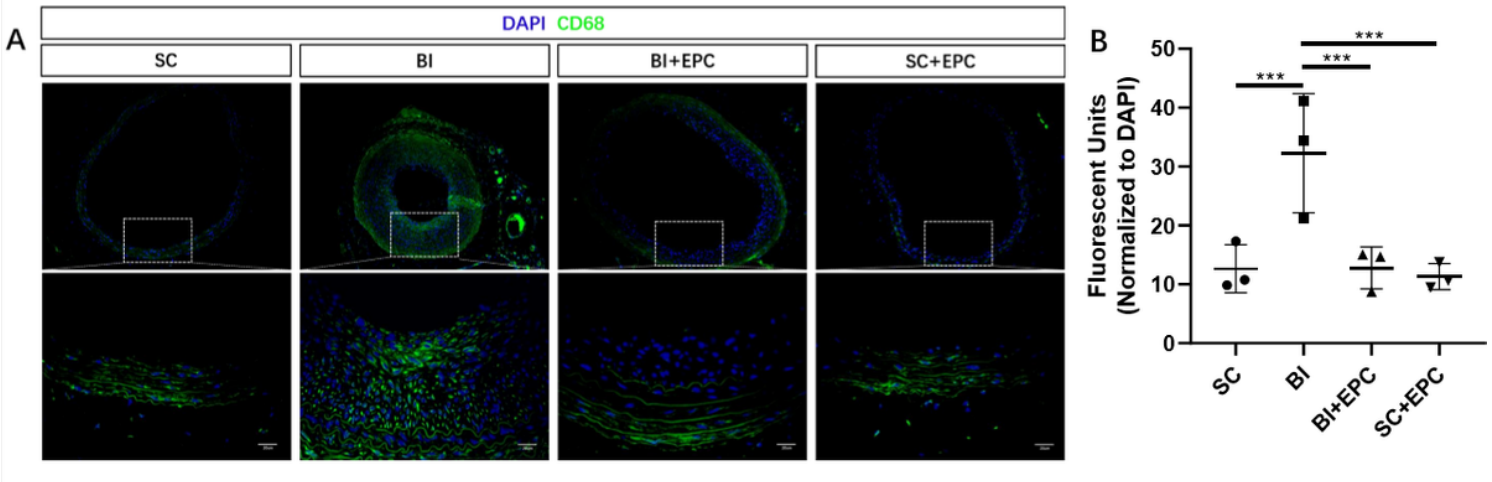

Figure 6

A-B Immunostaining of CD68 in carotid arteries of different groups. (A) CD68 staining of different groups. (B) Quantification of CD68 staining from images in (A); data shown as mean±SEM, analyzed by one-way ANOVA with LSD post-hoc comparisons, n=3. *No statistical difference, **P<0.05, ***P<0.01 vs BI group. SC=sham-operated control; BI=balloon injured; EPC&BI=EPC administration after balloon injured; EPC&SC=EPC administration after sham-operated.